Article 1

Directed Evolution of a Designer Enzyme Featuring an Unnatural Catalytic Amino Acid.

Researchers significantly enhanced the catalytic performance of a designer enzyme containing an unnatural amino acid (p-aminophenylalanine or pAF) through directed evolution.
Starting with an active designer enzyme (LmrR_pAF), they were able to identify key mutations that boosted the catalytic efficiency.

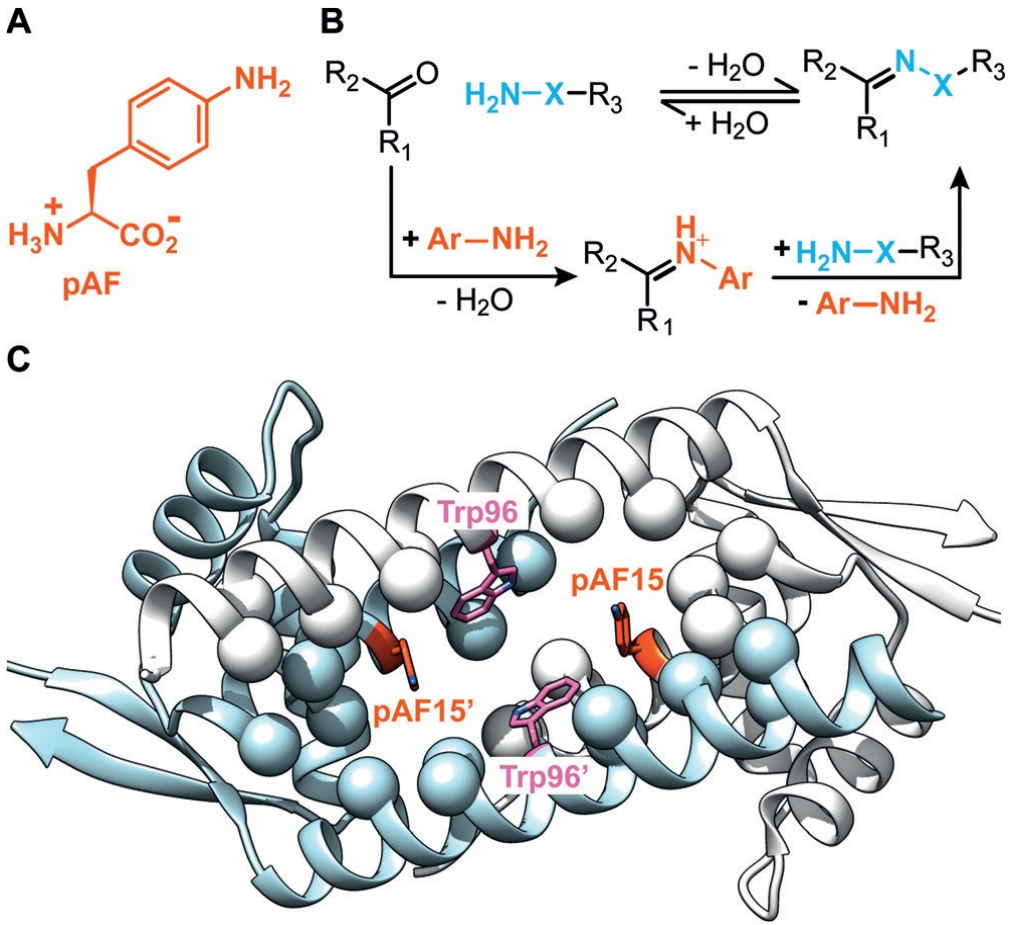

A. Chemical structure of p-aminophenylalanine (pAF) (p amino phenylalanine), the unnatural amino acid. It features a benzene ring with an amino group ($-NH_2$) at the para position, connected to the standard amino acid backbone.

•The catalytic mechanism showing iminium ion formation. This depicts how anilines accelerate hydrazone and oxime formation: The aniline's nitrogen (with its lone pair) attacks the carbonyl carbon of the aldehyde
•This forms a tetrahedral intermediate that collapses to an iminium ion
•The iminium ion is more electrophilic than the original aldehyde carbonyl
•This activated intermediate then reacts with either hydrazine (X=NH) or hydroxylamine (X=O) nucleophiles

p-Aminophenylalanine (pAF) is a modified version of phenylalanine where:
•The same standard amino acid backbone is preserved
•The benzene ring in the side chain has an amino group ($-NH_2$) added at the para position (the position opposite to where the methylene group connects to the ring)

•Crystal structure of the LmrR_pAF homodimer (PDB: 6I8N), showing: The catalytic aniline side chains in red
•Tryptophan 96 residues in pink
•The β-carbons of 13 additional residues that line the binding pocket shown as spheres

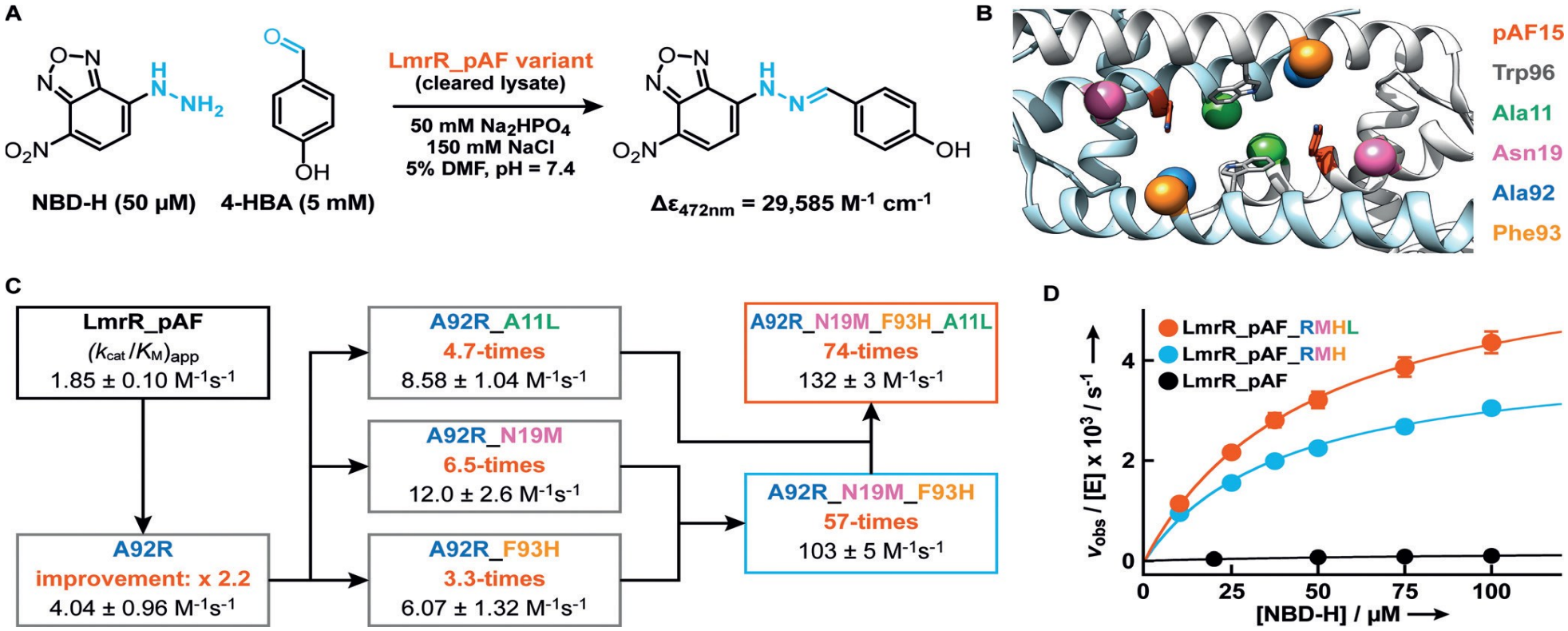

- **A**: The model reaction - hydrazone formation between NBD-H (4-hydrazino-7-nitro-2,1,3-benzoxadiazole) and 4-HBA (4-hydroxybenzaldehyde) in cell lysates.
- **B**: Close-up of the hydrophobic pore in LmrR_pAF
- β-carbons of positions that gave improved variants in rounds one and two as colored spheres
- **C**: Evolutionary optimization chart showing the apparent catalytic efficiencies of selected variants and their improvements compared to LmrR_pAF.
- **D**: Saturation kinetics comparison at 5 mM 4-HBA concentration for LmrR_pAF and the best variants after two rounds of directed evolution.

Detailed Chemical Mechanism

Methodology

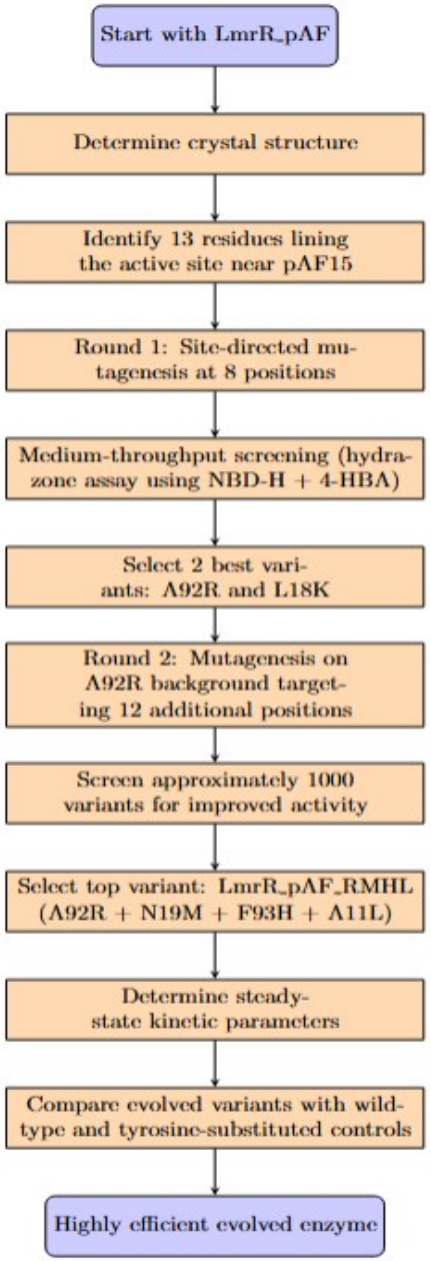

Results

LmrR_pAF_RMH
This variant contains three key mutations: A92R (R), N19M (M), and F93H (H).
Kinetic parameters:
•kcat = 4.53 × 10^-2 s^-1 (91-fold higher than LmrR_pAF)
•KNBD-H = 48 µM (lower than LmrR_pAF's 100 µM)
•K4-HBA = 46.4 µM (higher than LmrR_pAF's 7.92 µM)
•kcat/(KNBD-H × K4-HBA) = 20,500 M^-2 s^-1 (vs. 630 M^-2 s^-1 for LmrR_pAF)
•Effective molarity (EM) = 115 M (vs. 1.26 M for LmrR_pAF)
•Chemical proficiency (1/KTS°) = 5.2 × 10^7 M^-1 (vs. 1.6 × 10^6 M^-1 for LmrR_pAF)
•Improvement vs. aniline = 18,400-fold (vs. 560-fold for LmrR_pAF)
Critical dependency on the unnatural amino acid:
•When pAF15 was replaced with tyrosine in LmrR_pAF_RMH, it resulted in a 99.7% loss of catalytic efficiency

LmrR_pAF_RMHL
This variant contains four mutations: A92R (R), N19M (M), F93H (H), and A11L (L).
Kinetic parameters:
•kcat = 2.76 × 10^-2 s^-1 (55-fold higher than LmrR_pAF)
•KNBD-H = 49 µM (lower than LmrR_pAF's 100 µM)
•K4-HBA = 18.9 µM (higher than LmrR_pAF's 7.92 µM)
•kcat/(KNBD-H × K4-HBA) = 29,500 M^-2 s^-1 (vs. 630 M^-2 s^-1 for LmrR_pAF)
•Effective molarity (EM) = 69.8 M (vs. 1.26 M for LmrR_pAF)
•Chemical proficiency (1/KTS°) = 7.5 × 10^7 M^-1 (vs. 1.6 × 10^6 M^-1 for LmrR_pAF)
•Improvement vs. aniline = 26,500-fold (vs. 560-fold for LmrR_pAF)
Critical dependency on the unnatural amino acid:
•When pAF15 was replaced with tyrosine in LmrR_pAF_RMHL, it resulted in a 99.5% loss of catalytic efficiency

Results

1.Synergistic effect: The combination of N19M and F93H mutations was particularly crucial for the dramatic improvements observed.
2.Substrate scope: Both LmrR_pAF_RMH and LmrR_pAF_RMHL significantly accelerated hydrazone formation. Unlike the parent enzyme, both engineered variants could significantly accelerate hydrazone formation..
3.Overall catalytic proficiency: LmrR_pAF_RMHL achieved the highest catalytic efficiency, outperforming LmrR_pAF.
4.Reverting specific mutations: When either F93 or N19 was reverted to the original amino acid in these variants, there was a drastic loss of activity, highlighting their critical importance to the enhanced catalysis.

Article 2

Computation-guided engineering of distal mutations in an artificial enzyme

While previous engineering efforts typically focused on optimizing the active site chemistry, this work highlights the importance of protein dynamics and distal mutations in enhancing catalytic performance.

System Under Study

The researchers studied an artificial enzyme based on the lactococcal multidrug resistance regulator (LmrR) protein scaffold that was previously engineered to catalyze a hydrazone formation reaction using a non-canonical p-aminophenylalanine (pAF) residue.

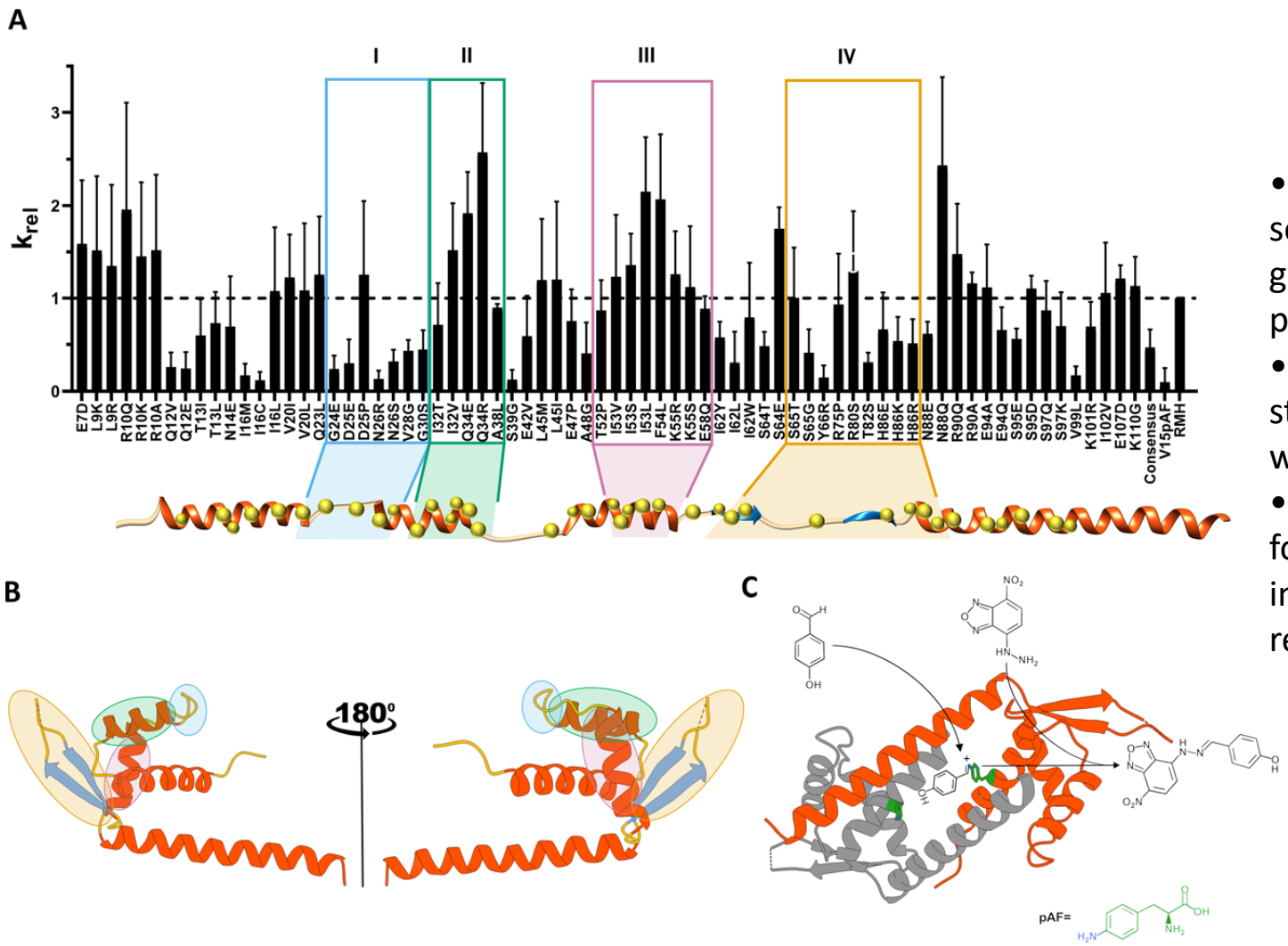

- A: The graph displays activity levels across the protein sequence with four distinct clusters (color-coded cyan, green, magenta, and yellow) that show different activity patterns.
- B: Illustrates these four clusters mapped onto the 3D structure of LmrR, showing their spatial distribution within the protein.
- C: Depicts the chemical reaction scheme for hydrazone formation between 4-HBA and NBD-H, including the iminium ion intermediate formed with the catalytic pAF residue.

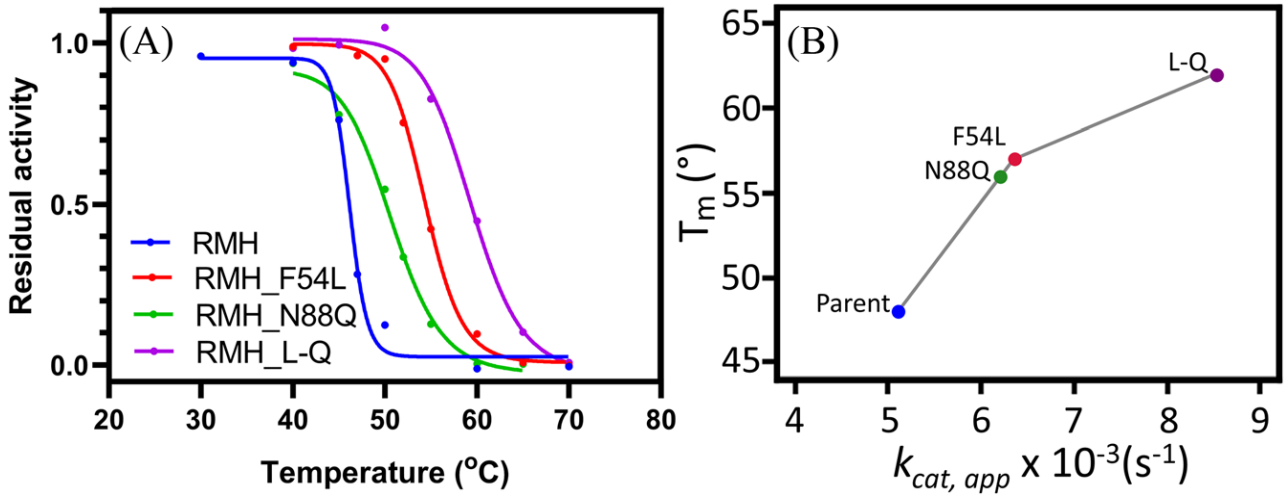

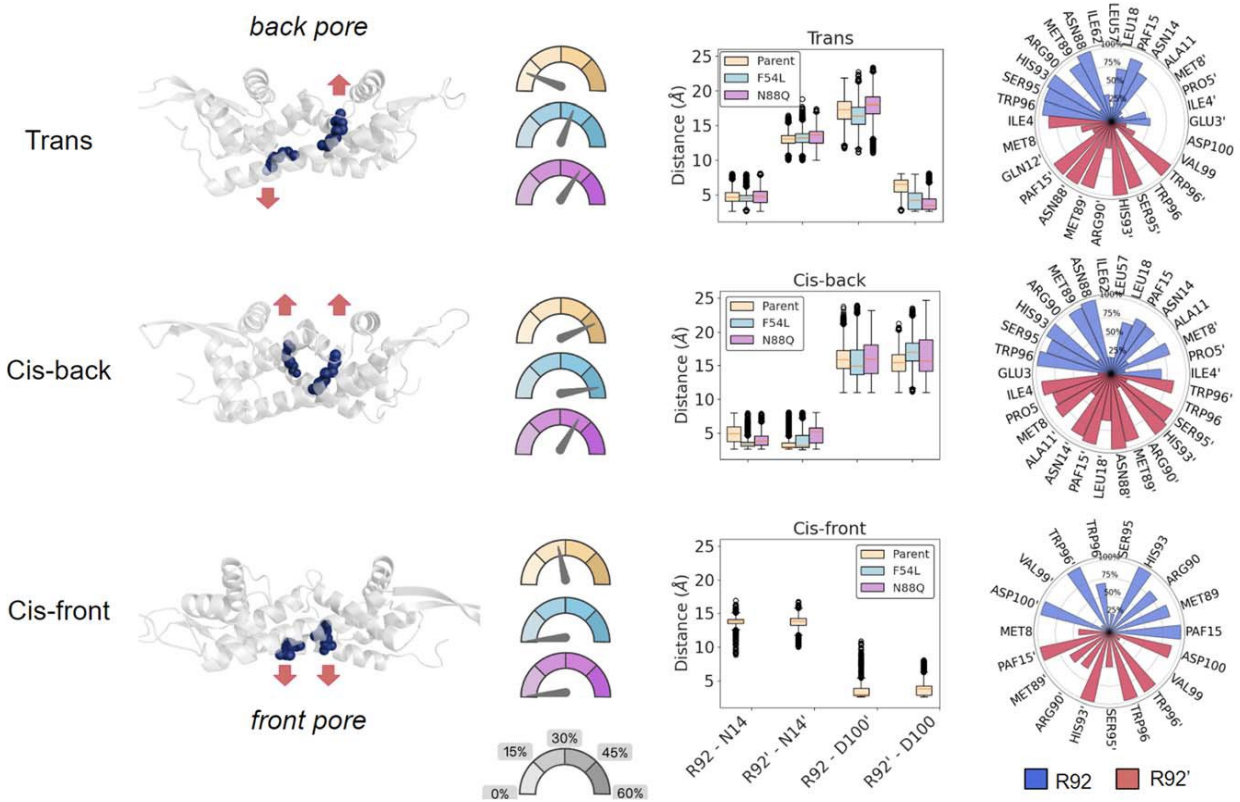

•A: Shows operational thermostability ($T10_{50}$) curves for the parent enzyme and the three variants (F54L, N88Q, L-Q), demonstrating how the mutations increase thermal stability.
•B: Correlates structural thermostability (Tm) with catalytic turnover rate (kcat), showing that the mutations improve both parameters simultaneously.

•Left: Displays representative structures of the three conformational states (trans, cis-back, cis-front) observed during MD simulations, focusing on the orientation of R92/R92'.
•Center: Contains gauge plots showing the percentage of time each variant spent in each conformation, plus box plots of distances used to identify the states.
•Right: Lists residues interacting with R92/R92' in each conformational state with their frequency of interactions.

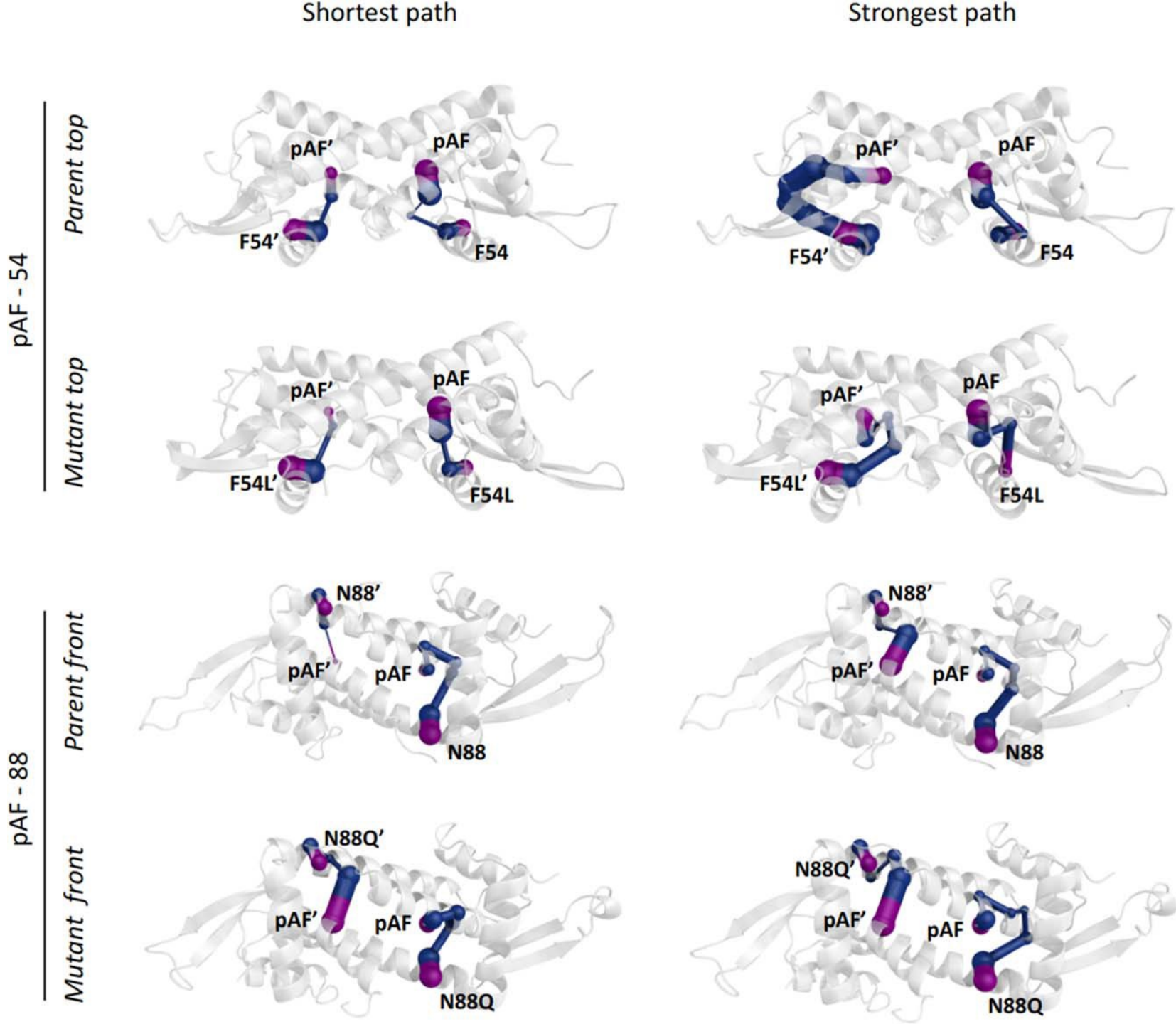

Shows allosteric pathways connecting the mutated positions (54/54' or 88/88') to the catalytic pAF based on dynamical network analysis. The left panels show the shortest paths, while the right panels show the strongest paths (weighted by betweenness).

Chemical Mechanism at Atomic Level

Methodology

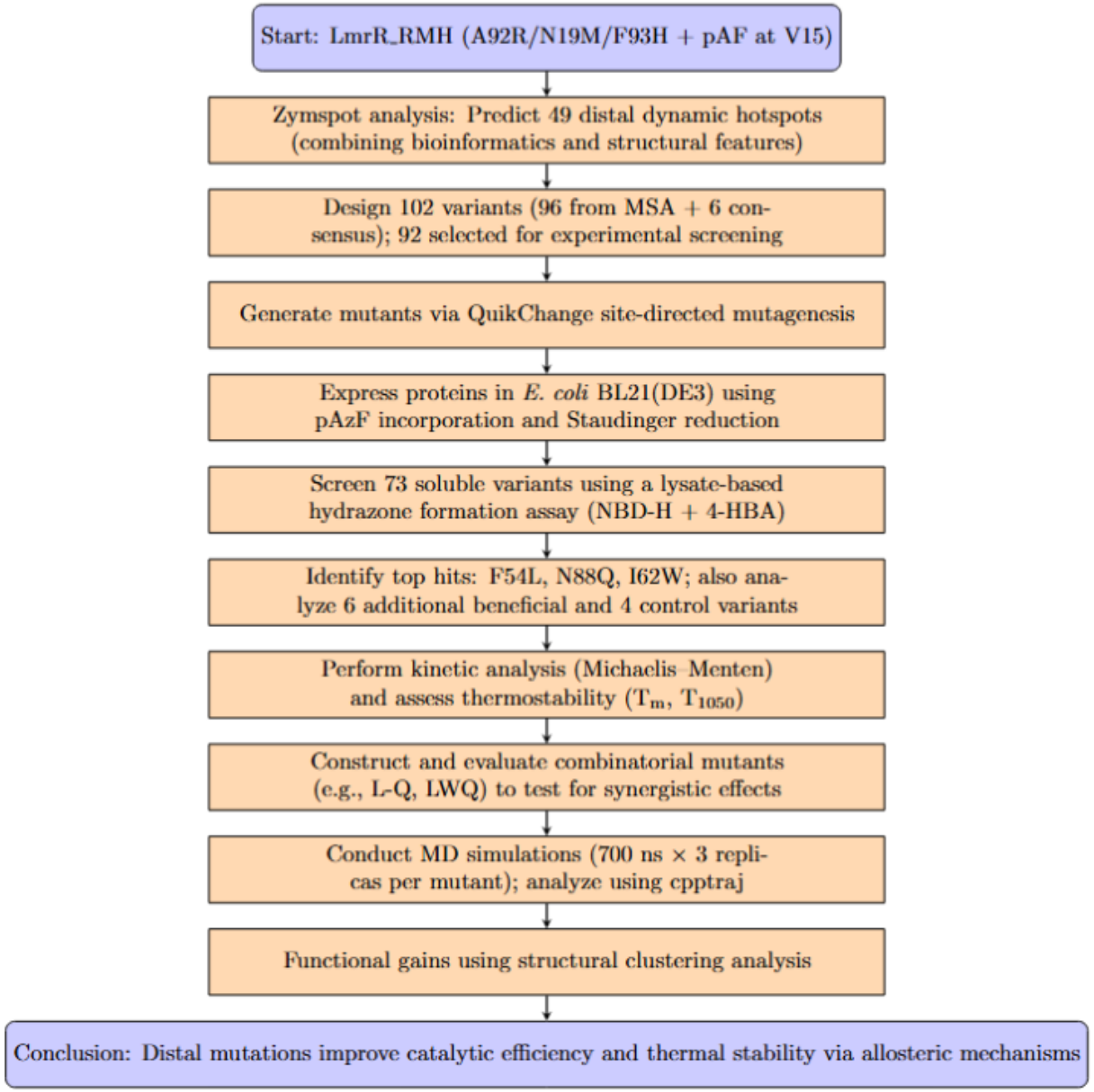

Results

- **Best Performing Variants**: Three single mutations located more than 11 Å from the catalytic pAF showed significant improvements:
- F54L
- I62W
- N88Q
- **Kinetic Characterization**: The N88Q mutation showed the most substantial improvement with a 1.6-fold increase in catalytic efficiency (kcat/KM) compared to the parent. This represented a 119-fold improvement over the original artificial enzyme.
- **Mutation Combinations**: The double mutant F54L_N88Q (LmrR_RMH_L-Q) showed a synergistic effect with:
- 66% higher turnover number (kcat)
- 14°C higher thermostability
- **Molecular Dynamics Insights**: The MD simulations revealed that these distal mutations affect the orientation of the key R92 residue, shifting the conformational ensemble toward catalytically productive states. Three main conformational states were identified based on R92/R92' orientation:
- "cis-back": Both R92/R92' pointing toward the back
- "trans": One pointing toward the entrance, one toward the back
- "cis-front": Both pointing toward the entrance (potentially catalytically inactive)

The beneficial mutations eliminated the "cis-front" conformation, which was hypothesized to be less catalytically productive.

- **Structural Effects**: The mutations resulted in:
- More compact protein structures (lower radius of gyration)
- Increased frequency of contacts in the hydrophobic pocket
- Alternative communication pathways between the mutation sites and the catalytic pAF

Article 3

Evolutionary Specialization of a Promiscuous Designer Enzyme

The paper investigates how a promiscuous designer enzyme evolves specialized catalytic activities. The authors previously created a designer enzyme by incorporating the non-canonical amino acid para-aminophenylalanine (pAF) into position 15 of the Lactococcal multidrug resistance regulatory (LmrR) protein. This modified enzyme (LmrR_pAF) showed promiscuous activity by catalyzing two distinct reactions:

Previous directed evolution campaigns had produced specialized variants for each reaction - with mutations that improved one activity while diminishing the other. This study aims to understand the molecular basis for this specialization.

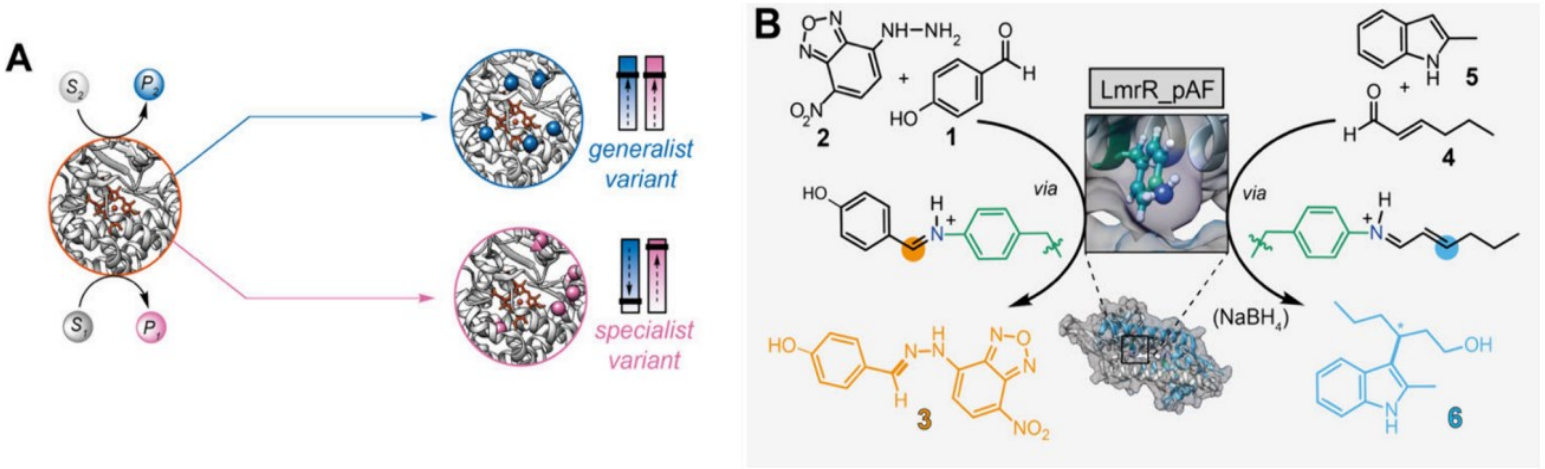

•**A**: Conceptual diagram showing how enzyme evolution can lead to either generalist variants (top, blue) that maintain multiple activities or specialist variants (bottom, pink) that excel at one reaction but lose other activities.

•**B**: Chemical mechanisms of the two reactions catalyzed by LmrR_pAF: hydrazone formation (top) and Friedel-Crafts alkylation (bottom), showing substrates, products, and the iminium ion intermediates.

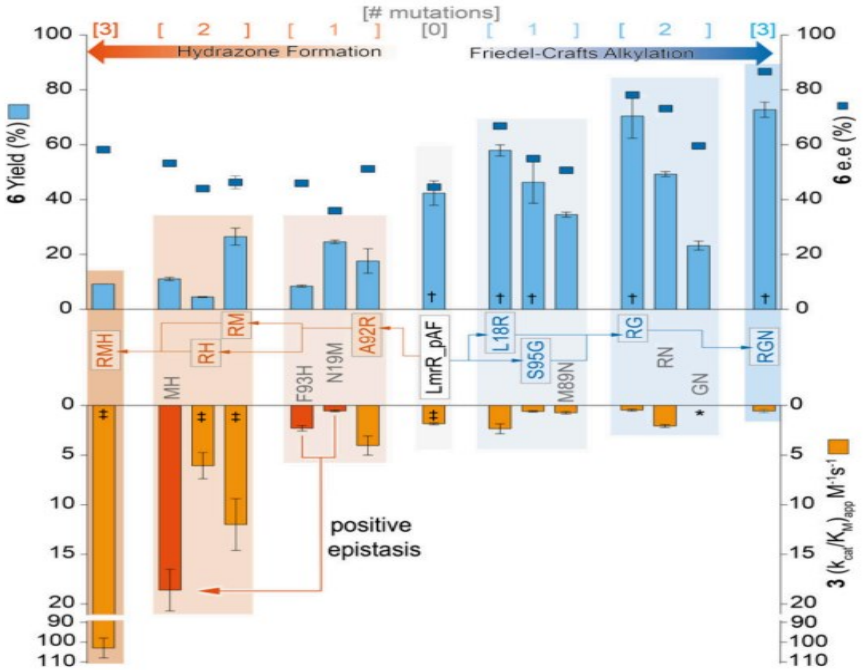

•Shows the evolutionary pathways mapped by testing all possible mutant combinations.
•Blue arrows track the Friedel-Crafts alkylation evolution path.
•Orange arrows track the hydrazone formation evolution path.

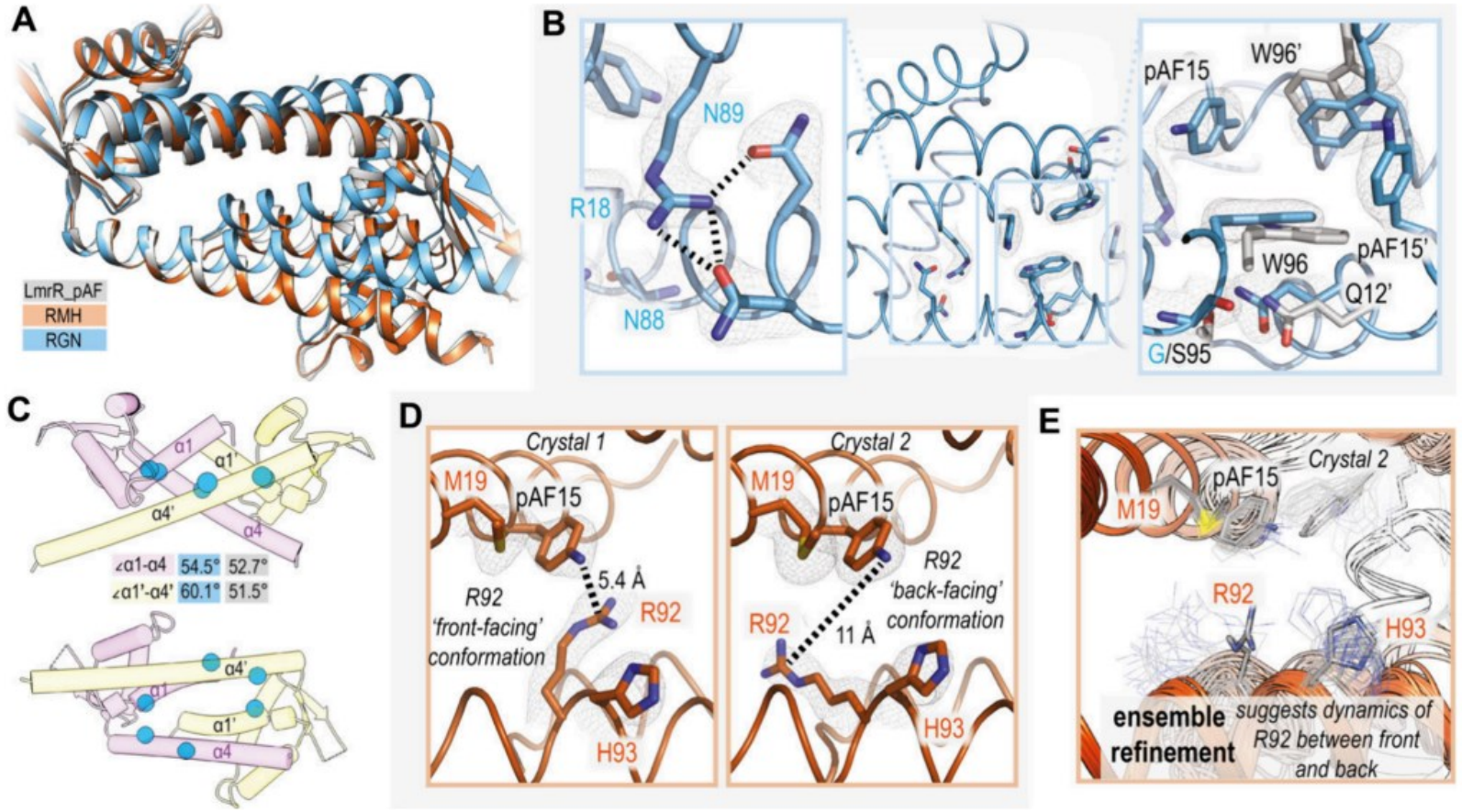

•**A**: Structural alignment of LmrR_pAF (gray) with RGN (blue) and RMH (orange) mutants, showing the significant structural change in RGN.
•**B**: Close-up of RGN mutations, highlighting new hydrogen bonding networks and decreased distances between key residues.
•**C**: Visualization of the altered angles between helices in RGN compared to parent enzyme.
•**D**: Active site of RMH in two different crystal structures, showing different conformations of the R92 side chain.
•**E**: Ensemble refinement results showing conformational flexibility of R92 in RMH.

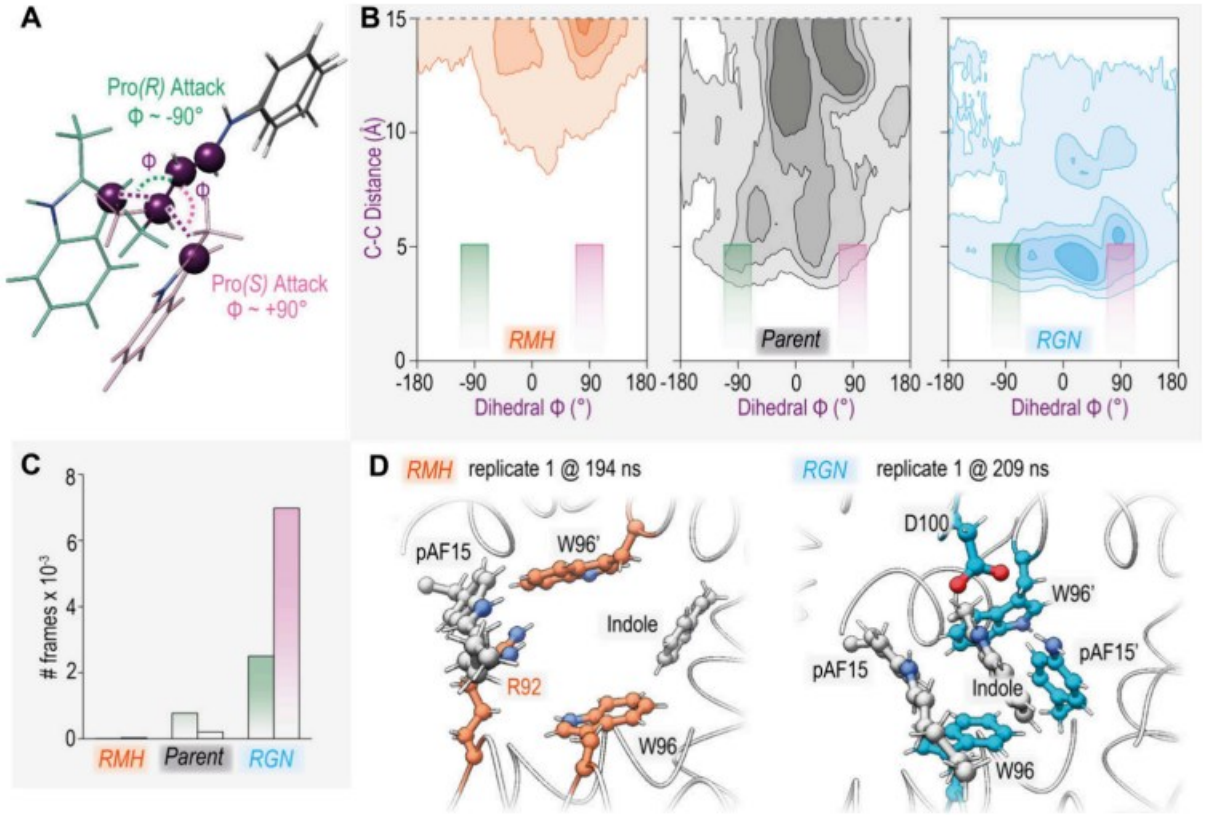

•**A**: Transition state models showing how dihedral angles determine product stereochemistry.
•**B**: Density plot of dihedral angles and distances from MD simulations, darker regions indicating more populated states.
•**C**: Count of near-attack conformations leading to (R) and (S) products in each variant.
•**D**: Representative frames from MD simulations showing substrate binding in RMH and RGN variants.

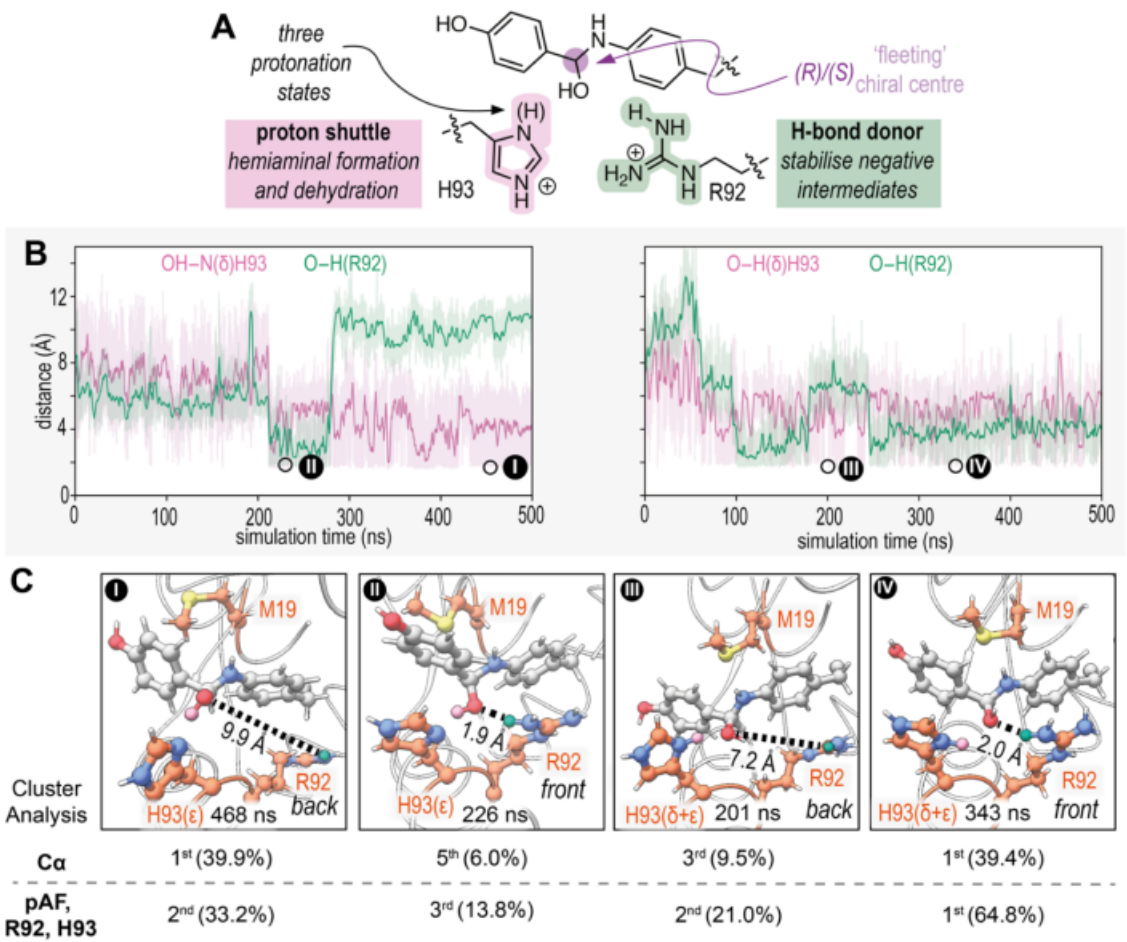

•**A**: Mechanistic hypothesis for how R92 and H93 assist in hemiaminal formation and dehydration.
•**B**: Distance measurements tracking hydrogen bonding interactions during MD simulations with different protonation states.
•**C**: Snapshots from simulations showing H93 and R92 participating in hydrogen bonding with reaction intermediates.

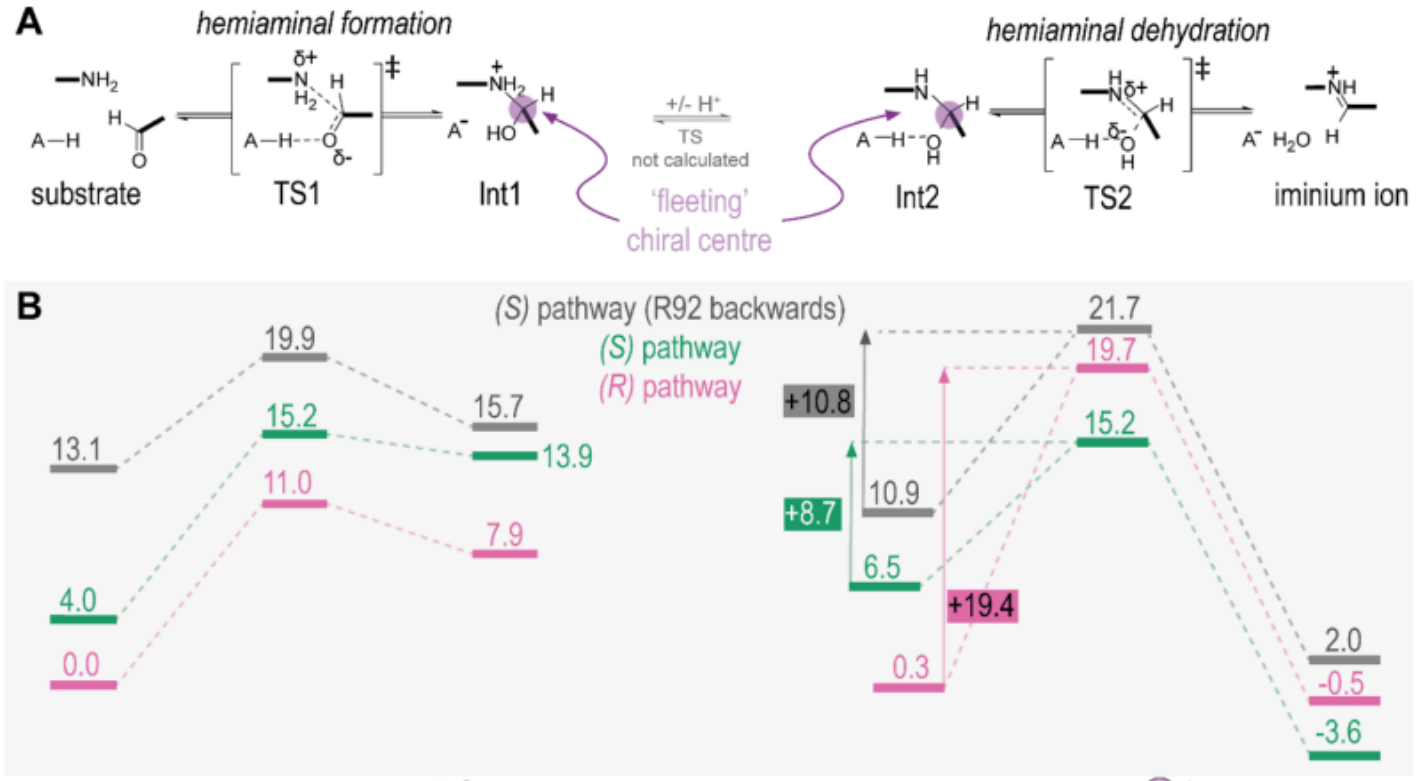

- **6A**: Detailed reaction mechanism for iminium formation via a hemiaminal intermediate.
- **6B**: Energy profiles for reaction pathways via (R) and (S) configured hemiaminals.
- **6C**: Overlaid structures of transition states with R92 in forward or backward conformations, showing key bond lengths.

Chemical Mechanism

Methodology

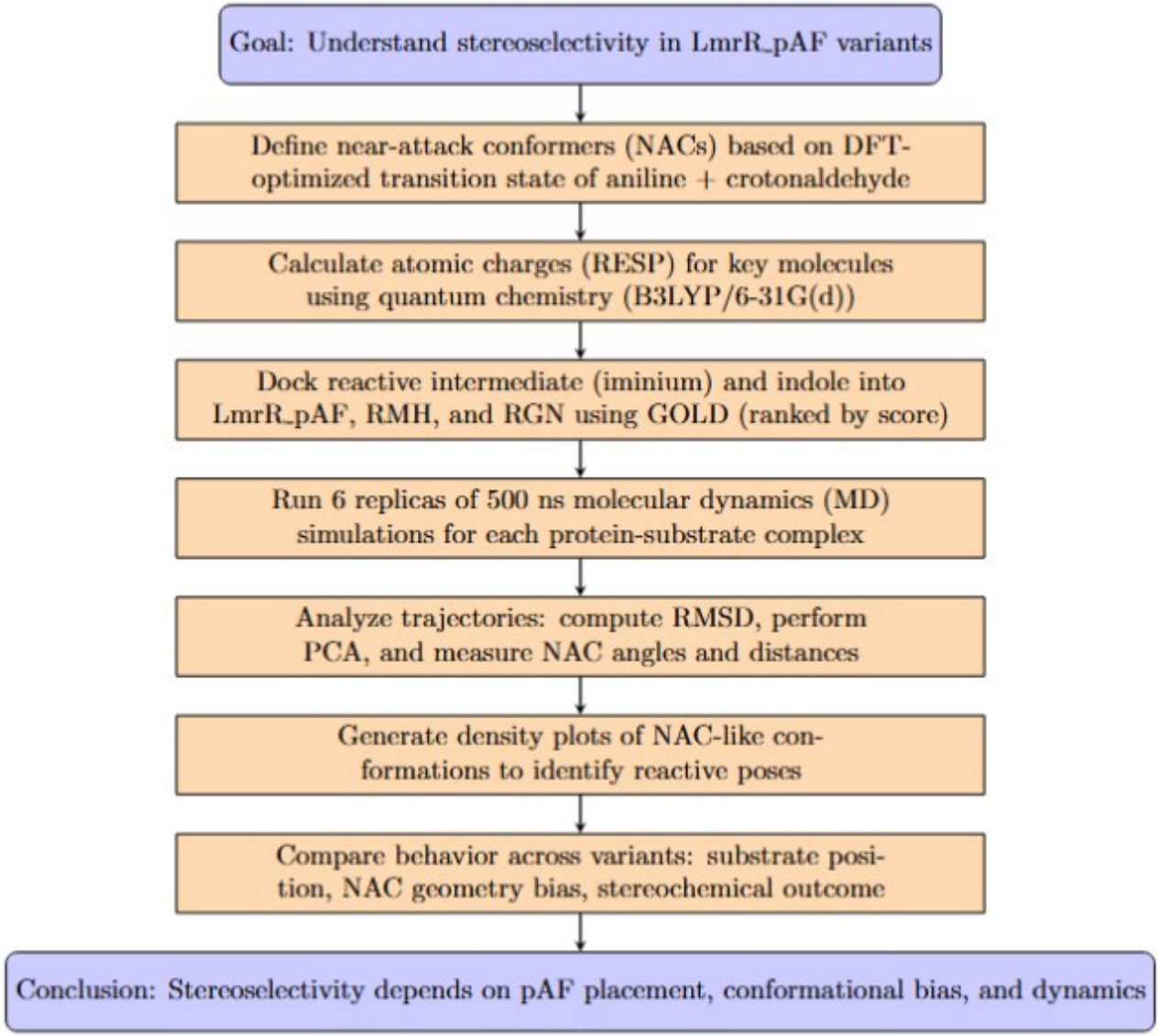

Results

Evolutionary Landscape Analysis

- Single mutations can cause significant activity loss (e.g., F93H decreases FC activity; S95G decreases HyF activity)
- Strong epistatic interactions observed between mutations (N19M and F93H show antagonism individually but synergy together)

Structural Changes in RGN (Friedel-Crafts Specialized)

- Dramatic change in quaternary structure with only three mutations
- New hydrogen bonding networks
- Closer packing of monomers creates an ideal binding site for indole substrates

Structural Changes in RMH (Hydrazone Formation Specialized)

- Overall structure remained similar to parent enzyme
- New catalytic residues (particularly R92 and H93) positioned near the pAF reactive site
- R92 shows conformational flexibility, with "forward-facing" conformers beneficial for catalysis

Computational Analysis of FC Reaction

- MD simulations showed better substrate retention in RGN compared to parent and RMH
- Clear bias toward forming the (S)-enantiomer in RGN variant
- Tighter W96/W96' arrangement in RGN creates ideal indole binding pocket

Conclusion

The study revealed how a promiscuous designer enzyme specialized through two distinct evolutionary pathways:

1. The Friedel-Crafts specialized variant (RGN) evolved through structural changes that altered the quaternary structure and pocket size, leading to improved substrate binding and stereoselectivity.
2. The Hydrazone formation specialized variant (RMH) evolved by creating a semisynthetic catalytic machinery where newly introduced amino acids (R92 and H93) work synergistically with the non-canonical pAF residue.

Article 4

Genetically encoded 3-aminotyrosine as catalytic residue in a designer Friedel–Crafts alkylase

This paper introduces the use of 3-aminotyrosine (aY) as a catalytic residue in a designer enzyme to catalyze the Friedel-Crafts (FC) alkylation reaction.

Previous work had utilized p-aminophenylalanine (pAF) for iminium ion catalysis, but this study explores 3-aminotyrosine as an alternative catalytic residue to investigate how the position of the catalytic amine group affects enzyme performance and selectivity.

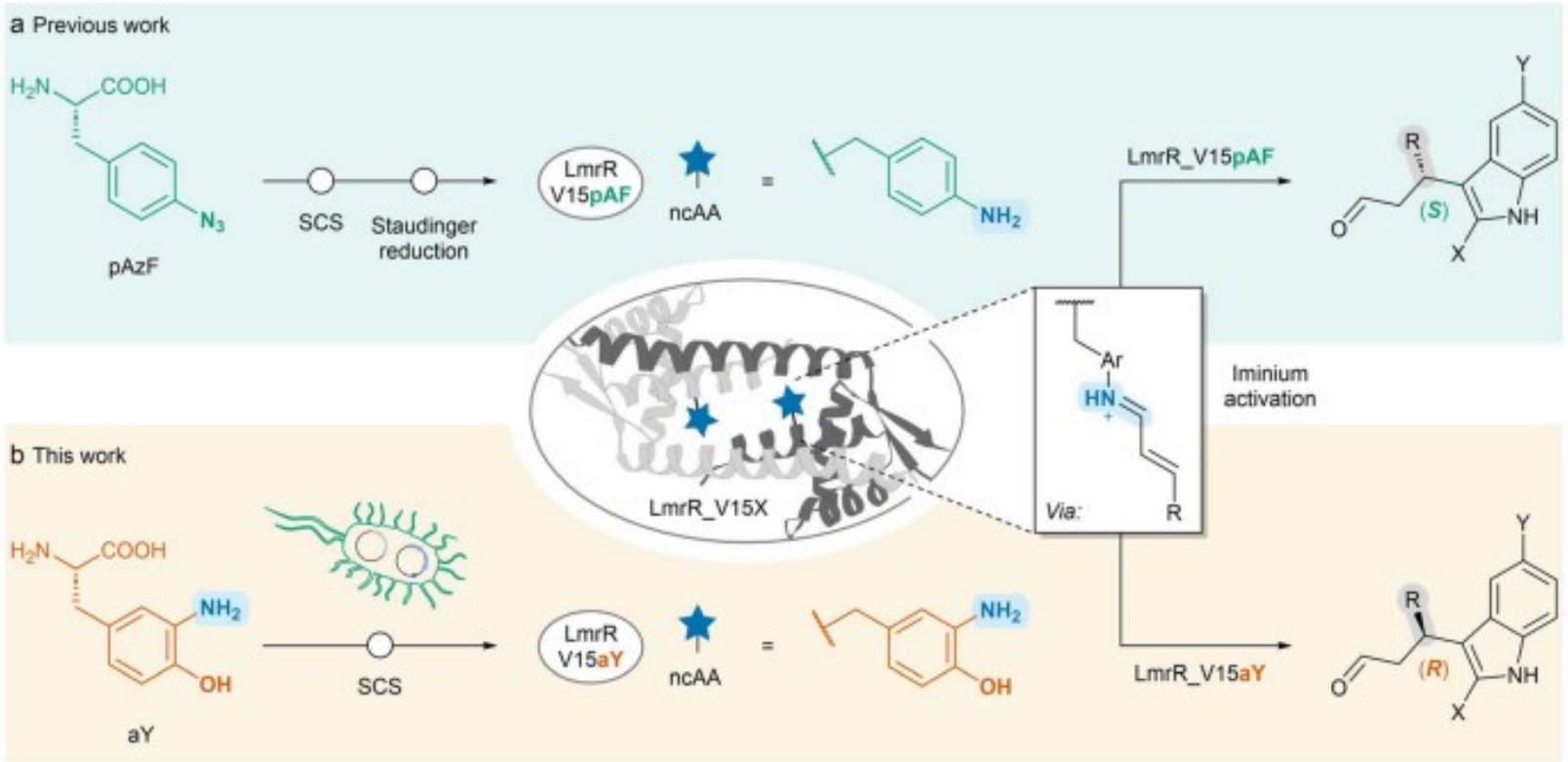

This scheme illustrates the creation of LmrR-based designer enzymes and their application in the FC-alkylation reaction:

•Part (a) shows the previous work incorporating pAzF (which is reduced to pAF) at position V15, which produces the (S)-enantiomer.

•Part (b) shows the current work with aY at position V15, which produces the (R)-enantiomer.

•The scheme illustrates the reaction between α,β-unsaturated aldehydes and indoles, highlighting the enantio-complementary of the two designs.

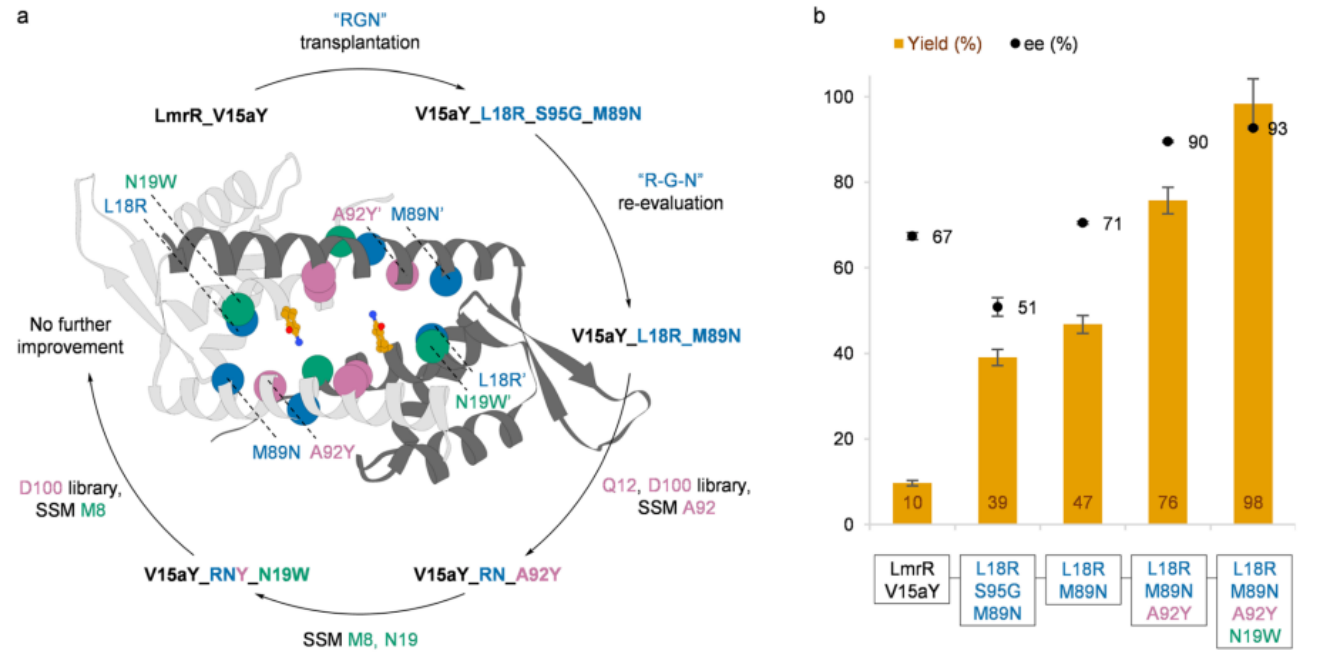

This figure shows the directed evolution process of V15aY for the FC-alkylation reaction.

- (a) displays the trajectory of the evolution campaign, with the positions targeted in each round shown as colored spheres on the crystal structure of LmrR_V15aY_RNYW. The orange structure represents the aY side chain.
- (b) presents a bar chart showing the analytical yield (gray bars) and enantiomeric excess (blue line) achieved by different variants during the evolution process, demonstrating the progressive improvement in both metrics.

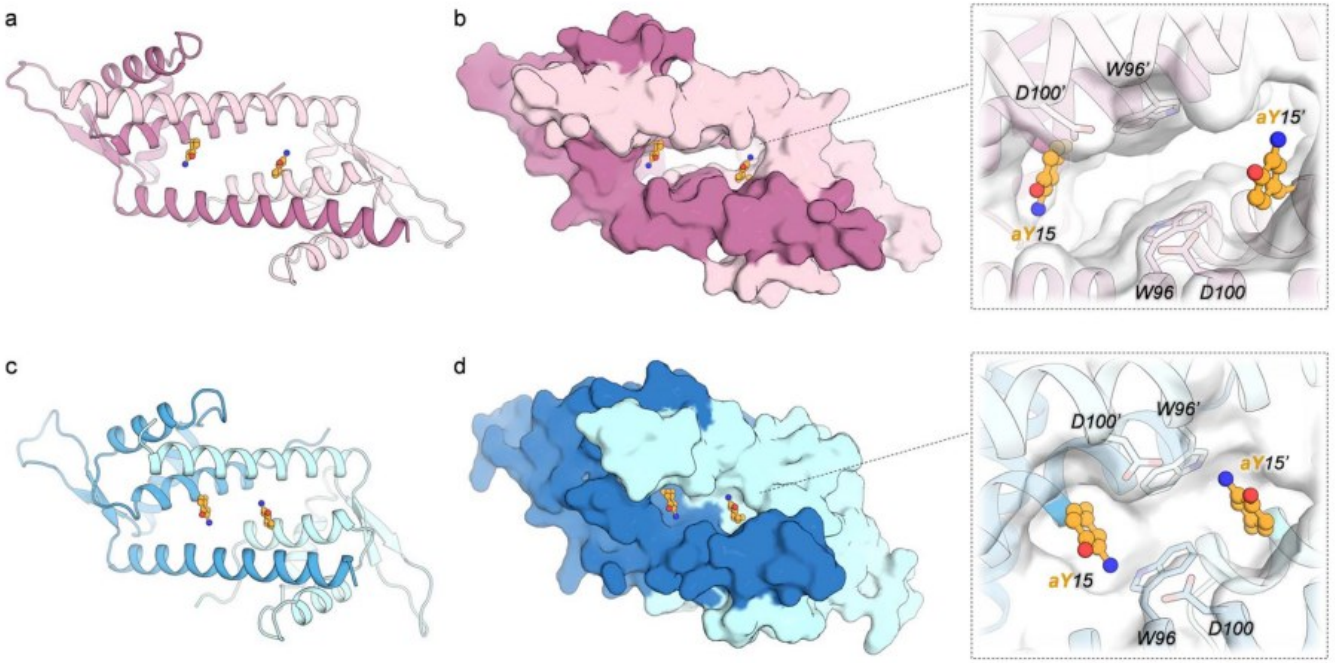

This figure compares the crystal structures of the parent enzyme (V15aY) and the evolved variant (V15aY_RNYW_KK):

- (a) and (c) show cartoon representations of the overall protein structures.
- (b) and (d) display surface representations with zoomed-in views of the dimeric interfaces, highlighting the aY residues at positions 15 and 15' shown as orange ball-and-stick models.
- The figure illustrates the narrowing of the active site pore in the evolved variant and the reorientation of the aY catalytic residue.

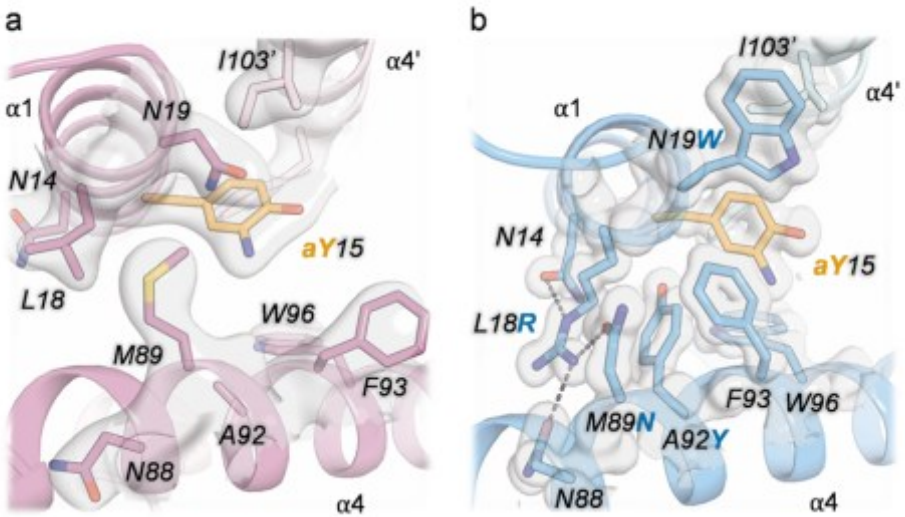

This figure provides close-up views of the crystal structures, highlighting key structural changes:

- (a) shows the parent enzyme V15aY.
- (b) shows the evolved variant V15aY_RNYW_KK.
- It illustrates how the mutations in the evolved variant (L18R, M89N, A92Y, N19W) create increased packing

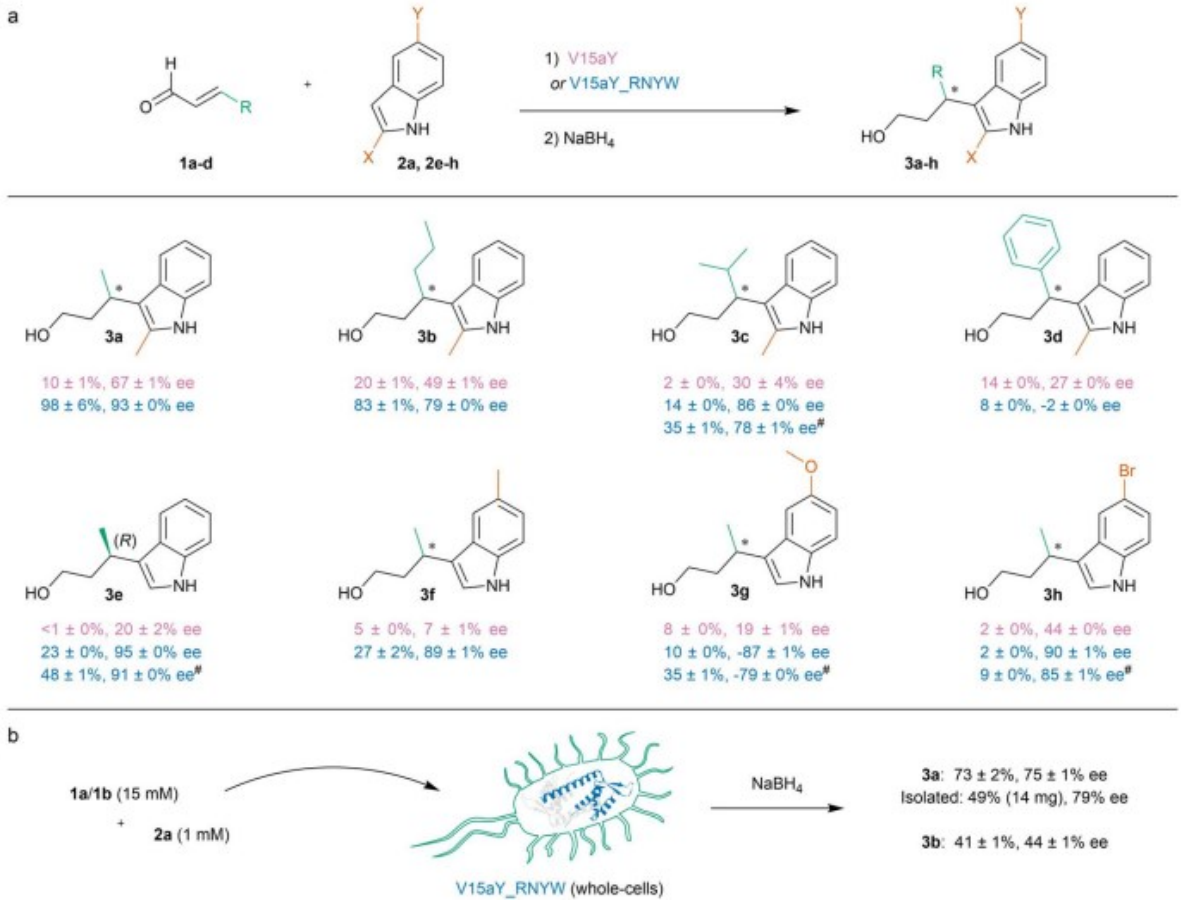

This scheme shows the substrate scope of the enzymes:

- Part (a) displays the various substrates tested with V15aY and V15aY_RNYW, showing yields and enantiomeric excesses.
- Part (b) illustrates the whole-cell catalysis approach and its application on a millimolar scale.

Chemical Mechanism

Results

Catalytic Performance:

1. V15aY successfully catalyzed the FC-alkylation with 67% enantiomeric excess (ee) but low yield (10%)
2. Most importantly, it produced the opposite enantiomer compared to V15pAF, demonstrating that the position of the amine group determined stereoselectivity

1.Directed Evolution:

1. The enzyme was evolved through multiple rounds to produce the quadruple mutant V15aY_RNYW (containing L18R, M89N, A92Y, N19W mutations)
2. The evolved enzyme showed dramatically improved performance: 98% yield and 93% ee
3. Kinetic analysis revealed a 3.4-fold increase in catalytic efficiency, primarily due to improved k_cat

2.Structural Analysis:

1. Crystal structures showed that the mutations caused a narrowing of the active site
2. The mutations reoriented the catalytic -NH_2 group from facing the side of the pore to pointing toward the center
3. Enhanced side chain packing for more closed active site configuration

3.Substrate Scope:

1. The enzyme showed good tolerance for various α,β-unsaturated aldehydes and indoles
2. The evolved enzyme achieved up to 95% ee with certain substrates
3. V15aY and V15pAF demonstrated complementary enantioselectivity for most substrates

4.Whole-Cell Catalysis:

1. The enzyme functioned effectively in whole-cell catalysis without cell lysis or purification
2. Preparative scale reaction (0.14 mmol) yielded 49% isolated yield with 79% ee

Conclusions

1.Simply changing the position of the catalytic amine group from para (in pAF) to meta (in aY) inverted the enantioselectivity of the reaction.
2.Directed evolution significantly improved the enzyme's performance, resulting in a highly efficient and selective artificial FC-alkylase.
3.The evolved V15aY_RNYW and the previously developed V15pAF_RGN form a set of enantio complementary FC-alkylases that can produce either enantiomer of the products with high selectivity.

Methodology